PERFORMANCE OF DOWEL BARS AND RIGID PAVEMENT

Final Report

For

FEDERAL HIGHWAY ADMINISTRATION
U.S. DEPARTMENT OF TRANSPORTATION

By

Shad M. Sargand
Russ Professor
Department of Civil Engineering
Ohio University

Ohio University
Ohio Research Institute for Transportation and the Environment
Department of Civil and Environmental Engineering
Athens, Ohio

June, 2001

1. Report No.	2. Government Accession No.	3. Recipient's Catalog No.
FHWA/HWY-01/2001		

4. Title and Subtitle	5. Report Date
Performance of Dowel Bars and Rigid Pavement	June 2001
	6. Performing Organization Code
	8. Performing Organization Report No.
7. Author(s)	
Shad M. Sargand	10. Work Unit No. (TRAIS)
9. Performing Organization Name and Address	11. Contract or Grant No.
Ohio University 114 Stocker Center Athens, Ohio 45701-2979	State Job No. 14667(0)
	13. Type of Report and Period Covered
	Final Report
12. Sponsoring Agency Name and Address	14. Sponsoring Agency Code
Ohio Department of Transportation 1980 W Broad Street Columbus, OH 43223	

15. Supplementary Notes

16. Abstract

In 1997, an experimental high performance jointed concrete pavement was constructed on US 50 east of Athens, Ohio. In this pavement, 25% of the Portland cement was replaced with ground granulated blast furnace slag. Epoxy-coated steel dowel bars were used throughout most of the project to provide load transfer across the joints to adjacent slabs. Fiberglass dowels and stainless steel tubes filled with concrete were installed in a few joints to compare their effectiveness with the epoxy-coated bars. A limited number of epoxy-coated steel and fiberglass bars were instrumented with strain gauges to measure bending moments and vertical shear induced in the bars as the concrete cured, during environmental cycling of moisture and temperature in the concrete slab, and as Falling Weight Deflectometer applied dynamic loads near the pavement joints. Thermocouples were installed to monitor temperature at different depths in the concrete layer during the strain measurements. The strain data indicated that: 1) significant stresses were generated in the dowel bars and in the concrete surrounding the dowel bars soon after the concrete was placed, 2) temperature gradients in the concrete slabs caused high stresses in the bars, and 3) stress levels generated in the fiberglass dowel bars were less than those generated in the epoxy-coated steel bars.

17. Key Words	18. Distribution Statement
High performance concrete pavement; ground granulated blast furnace slag; epoxy-coated steel dowel bars; fiberglass dowel bars; dowel bar stress; curing; dynamic loading;	No Restrictions. This document is available to the public through the National Technical Information Service, Springfield, Virginia 22161

19. Security Classif. (of this report)	20. Security Classif. (of this page)	21. No. of Pages	22. Price
Unclassified	Unclassified		

Table of Contents

Preceding Page Blank

List of Tables

List of Figures

CHAPTER 1

INTRODUCTION

1.1 General Statement

The economic burden associated with repairing and maintaining existing highway pavements is rapidly consuming an increasingly significant portion of the annual transportation budget. One of the major areas of concern is the repair of rigid pavements resulting from premature distress at transverse contraction joints.

The performance of Portland cement concrete joints in transferring traffic loads to adjacent slabs is influenced by several factors, including temperature and moisture distributions within the slabs, physical properties of the base and subgrade underlying the pavement, moisture content of the subgrade, and the type, size and spacing of dowel bars. Finite element methods have been used with some success in analyzing concrete pavement systems containing joints and cracks. The accuracy of these methods, however, depends upon how realistically the properties of the concrete and subgrade, the dowel-concrete interaction, and traffic loading can be modeled. These procedures must then be verified and calibrated with data obtained on in-service pavements. To date, stresses induced in dowel bars and concrete slabs from environmental cycling and dynamic loading have not been determined in the field.

1.2 Background

During the construction of concrete pavements, transverse contraction joints are sawed at specified intervals to control shrinkage cracking and to allow for slab deformations caused by temperature and moisture cycles. These joints, however, introduce discontinuities into the pavement structure and serve as sources for premature distress. Researchers and engineers such as Ozbeki, et al. (1) found that the most severe deterioration of rigid pavement occurs at these joints.

Circular steel dowel bars have been the preferred method of transferring vertical shear and horizontal bending moments to adjacent slabs (2). These bars must be properly aligned longitudinally and lubricated over half of their length prior to placement of the concrete, so as not to lock the slabs together and restrict horizontal expansion and contraction. Vertical deformation of the slab ends is restricted in accordance with the stiffness of the dowel bars. The design of dowels is based on an analysis presented by Timoshenko (3) who assumed that individual bars behave like a beam on a Winkler-type elastic foundation. Basing his research on the theory proposed by Timoshenko, Friberg (4) was the first to study the behavior of dowel bars as a group. He also examined the effects of dowel bar diameter and spacing.

Tabatabaie-Raissi (5) developed a three-dimensional finite element program to analyze the behavior of dowel bars and concrete at transverse rigid pavement joints. His study indicated that the diameter of the dowel bars and the concrete modulus of elasticity have significant effects on joint performance. While he recommended his model for the design of standard joints on new

rigid pavement, he did not suggest it be used for undercut joints or other types of joint repairs on rehabilitated pavements.

In a 1987 study conducted by Vyce (6), the New York Department of Transportation monitored the long-term performance of several load-transfer devices (LTDs) in rigid pavement joints, including fiberglass dowel bars, steel dowel bars, and steel I-beams. The study consisted of observing LTD performance in the field and conducting pullout tests in the laboratory. Conclusions on the LTDs tested were:

1. All LTD designs were durable over the 12 to 15 year study period.

2. Pullout resistance was a function of the LTD type, with the I-beam devices providing the least resistance. LTDs welded to a basket assembly offered the most resistance to axial loading.

1.3 Objectives

Theoretical studies, field observations, and laboratory tests are all helpful in understanding the impact of different variables on dowel bar performance. Actual dowel bar response needs to be measured under traffic type loading, and these data must be combined with laboratory data to validate theoretical models.

The general purposes of this study were to evaluate dowel response under a variety of loading and environmental conditions in the field, and to compare the measured responses of different types of dowel bars. Specific objectives included the following:

1. Instrument standard steel and fiberglass dowel bars for the monitoring of strain induced by curing, changing environmental conditions and applied dynamic forces.

2. Install these dowel bars in an actual PCC pavement at the time of construction.

3. Record strain measurements periodically over time to determine forces induced in the dowel bars during curing and during changing environmental conditions.

4. Record strain measurements in the dowel bars as dynamic loads are applied with the Falling Weight Deflectometer (FWD).

5. Evaluate strain histories recorded for this in-service pavement.

CHAPTER 2

SITE LOCATION AND MATERIAL PROPERTIES

2.1 Site Location

As part of the Federal Highway Administration (FHWA) project TE-30, "High Performance Rigid Pavements", the Ohio Department of Transportation (ODOT) constructed an experimental Portland cement concrete (PCC) pavement containing 25% ground granulated blast furnace slag (GGBFS) on U.S. 50, approximately five-miles east of the city of Athens, Ohio and across from Dow Lake. Fiberglass and hollow stainless steel dowel bars filled with concrete were added to a portion of the project, and a few fiberglass and standard steel bars were instrumented to measure strain during curing, environmental cycling, and Falling Weight Deflectometer (FWD) loading. Instrumentation of the dowels was completed in late September of 1997, while placement of the dowels and concrete in the eastbound lanes occurred on October 14, 1997. The westbound lanes were placed in the summer of 1998. The FHWA awarded Ohio University a contract to evaluate the response of the instrumented dowel bars and this report summarizes the results of that study.

2.2 Pavement Design

The U.S. 50 pavement was constructed of high performance (HP) reinforced concrete 254 mm (10 in) in thickness, with two 3.66 m (12 ft.) wide lanes in each direction and a joint spacing of 6.4 m (21 ft.). W8.5 x W4 – 6 x 12 welded wire mesh was added to minimize the effects of any unexpected midslab cracking. Dowel bars 38 mm (1.5 in) in diameter and 457 mm (18 in) long were located 305 mm (12 in) on centers at the joints. The 3.05 m (10 ft.) wide outside shoulder and 1.22 m (4 ft.) wide inside shoulder were constructed of plain concrete. The pavement was placed on a 102 mm (4 in) thick 307 New Jersey non-stabilized drainage base (NSDB) and a 152 mm (6 in) thick 304 dense graded aggregate base (DGAB) with a bituminous prime coat applied at 1.81 l/m^2 (0.4 gal/yd^2) between the two base materials.

2.3 P.C. Concrete Mix Design

The high performance concrete mix consisted of Type I cement, ground granulated blast furnace slag replacing 25% of the cement, water reducer and air entraining admixtures, natural concrete sand fine aggregate, and #8 gravel coarse aggregate. The water/cement ratio for the mix was 0.446. Weights of various components of the mix were as follows:

Table 2.1 – Concrete Mix Design

High Performance Concrete Mix Design	
Component	Weight per cubic meter
Fine Aggregate	647.7 Kg (1428 lbs.)
Coarse Aggregate	619.2 Kg (1365 lbs.)
Cement	186.9 Kg (412 lbs.)
Water	143.3 Kg (316 lbs.)
GGBF Slag	62.6 Kg (138 lbs.)
Total Weight	1659.7 Kg (3659 lbs.)
Water Reducer Admixture	56.7 g/cwt (2 oz/cwt)
Air Entrainment Admixture	119.1 g/cwt (4.2 oz/cwt)

2.4 Physical Properties of P.C. Concrete

Laboratory tests were performed on samples of the concrete mix used in the pavement, including compression, beam flexure, and split tensile tests. The results of these tests are given in the table below. The slump of the concrete was 51 mm (2 in) and the air content was 8.2 %.

Table 2.2 – Laboratory Test Results for HP Concrete

Unit Weight	134.6 pcf (2,155 kg/m^3)
Compressive Strength @ 7 days Compressive Strength @ 22 days Compressive Strength @ 28 days	20.0 MPa (2,900 psi) 26.2 MPa (3,800 psi) 27.6 MPa (4,000 psi)
Split Tensile Strength @ 28 days	2.48 MPa (360 psi)
Rupture Modulus @ 28 days	2.76 MPa (400 psi)*
Static Modulus of Elasticity @ 28 days	25.92 GPa (3.76 x 10 ^{6} psi)

*Test specimens cured on site during cool weather.

2.5 Physical Properties of Base

The 304 DGAB and 307 New Jersey base materials used on this U.S. 50 project met the ODOT gradations specified in Table 2.3. Resilient moduli of the 307NJ subbase were determined using AASHTO procedures and the results are shown in Table 2.4.

Table 2.3 - Sieve Analysis Specification for Aggregate Base

Item 304 (DGAB)		307 New Jersey Base	
Sieve Size	Total % Passing	Sieve Size	Total % Passing
50 mm (2 inch)	100	38 mm (1-1/2 inch)	100
25 mm (1 inch)	70 - 100	25 mm (1 inch)	95 – 100
19 mm (3/4 inch)	50 - 90	12.5 mm (1/2 inch)	60 - 80
4.75 mm (No. 4)	30 - 60	4.75 mm (No. 4)	40 - 55
600 μm (No. 30)	9 - 33	2.36 mm (No. 8)	5 - 25
75 μm (No. 200)	0 - 13	1.18 mm (No. 16)	0 - 8
		300 μm (No. 50)	0 - 5

Table 2.4 –Resilient Modulus Results on 307 NJ Base Material

Deviatoric Stress	Resilient modulus
17.2 KPa (2.5 psi)	27.59 MPa (4002 psi)
34.4 KPa (5.0 psi)	40.45 MPa (5867 psi)
68.9 KPa (10.0 psi)	59.34 MPa (8606 psi)
103.4 KPa (15.0 psi)	72.25 MPa (10,769 psi)
137.9 KPa (20.0 psi)	87.07 MPa (12,628 psi)

2.6 Physical Properties of Dowel Bars

The mechanical properties of dowel bars installed on this project were evaluated in the laboratory and these data were used in the determination of forces generated during FWD loading and environmental cycling. Properties of the steel dowel bars were as follows:

Young's Modulus (E) = 207 GPa (30 x 10^6 psi.)

Shear Modulus (G) = 78 GPa (11.3 x 10^6 psi.)

The fiberglass dowels supplied by RJD Industries, Inc., were pultruded and composed of "E" type continuous fiberglass filaments bonded together by a blended unsaturated isophthalic polyester resin. The dowels were considered to be a transversely isotropic media and their composition gave them different mechanical properties in the directions parallel and perpendicular to the longitudinal axis of the bar. Properties of the fiberglass dowels were:

Modulus of Elasticity $E_{longitudinal}$ = 55 GPa (8 x 10^6 psi.)

Modulus of Elasticity $E_{transverse}$ = 13.75 GPa (2 x 10^6 psi.)

Shear Modulus $G_{transverse}$ = 2.82 GPa (0.41 x 10^6 psi.)

Poisson's Ratio $\upsilon_{longitudinal}$ = 0.071

Poisson's Ratio $\upsilon_{transverse}$ = 0.42

CHAPTER 3

INSTRUMENTATION AND DATA COLLECTION

3.1 Dowel Bar Instrumentation

The three types of dowels used on the U.S. 50 research project included standard epoxy-coated steel, fiberglass, and 304 stainless steel tubes filled with concrete. The steel and fiberglass dowels had a diameter of 38.1 mm (1.5 in). The concrete-filled stainless steel bars had an outer diameter of 38.1 mm (1.5 in) and an inner diameter of 34.3 mm (1.35 in). All bars were 457.2 mm (18 in) long.

A flat area was cut for each of three gages mounted at the center of the instrumented standard steel and fiberglass bars. A shallow groove was cut along the length of the bar to protect the lead wires coming from the gages to the end of the bar. This helped protect the sensors while minimizing the effect of their presence on the stiffness of the bars. At the end of each dowel, a small chamber was cut to allow the lead wires to be epoxied so they would not be exposed to the concrete (see Figures 3.1 and 3.2). The stainless steel dowels were not instrumented because the thin wall thickness did not permit the machining of a flat surface or the cutting of a groove for the wires.

Each instrumented dowel bar contained a uniaxial strain gage on the top and the bottom, and one 45-degree rosette on the side. The uniaxial gages measured environmental and dynamic strain while the rosette gages measured only dynamic strain. All gages had a resistance of 120-ohms and were mounted at the center of the bar. The strain gages were either welded or cemented to the bars with epoxy, and coated with Nitrile M-coat B protective epoxy. Aluminum tape was placed over the coating to help ensure a good bond and minimize the intrusion of water. The two uniaxial gages were wired in a half-gage configuration, so as to arithmetically sum strain measured on the top and bottom of the dowel bars by subtracting the top gage output from the bottom gage output. This total strain was halved to determine the average strain at each gage. The rosette gages were wired in a quarter-gage configuration and monitored individually.

Before welding the bars to the baskets, care was taken to ensure the gages on each bar were lined up vertically and the bars were properly aligned transversely along the basket. The baskets were then located where transverse contraction joints would be sawed directly over the gages shortly after placement of the concrete, since maximum strain in the bars will occur where the transverse crack propagating downward from the saw kerf intersects the bars.

Each dowel test section consisted of six consecutive joints containing a particular type of dowel, with the middle two baskets containing the instrumented bars. Three dowel bars were instrumented in each of the two baskets, with the remainder of the bars containing non-instrumented bars of the same type. The instrumented bars were placed 152.4 mm (6 in), 762 mm (30 in), and 1.98 m (78 in) from the outside edge of the pavement, as shown in Figure 3.3. The wheelpath dowel (762 mm or 30 in) was monitored most closely, since it was assumed to be in the area of maximum dowel bar stress during actual traffic loading.

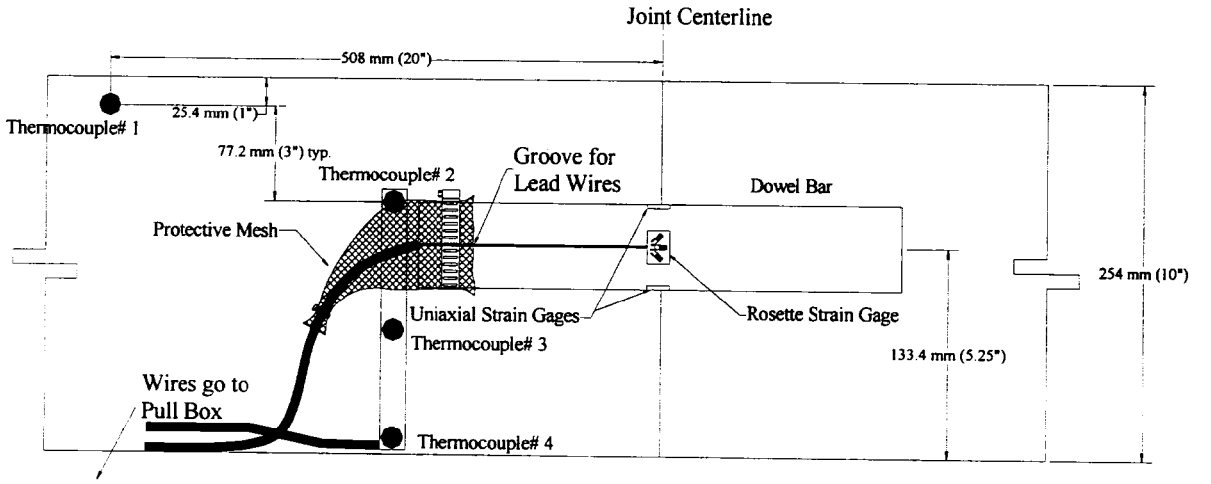

Figure 3.1 – Side View of Dowel and Thermocouple Placement in Slab

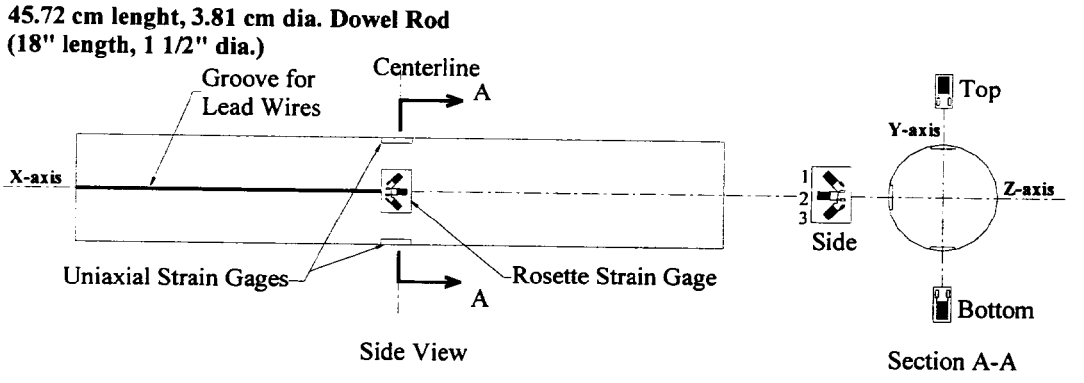

Figure 3.2 – Strain Gage Installation Plan for Dowel Bars

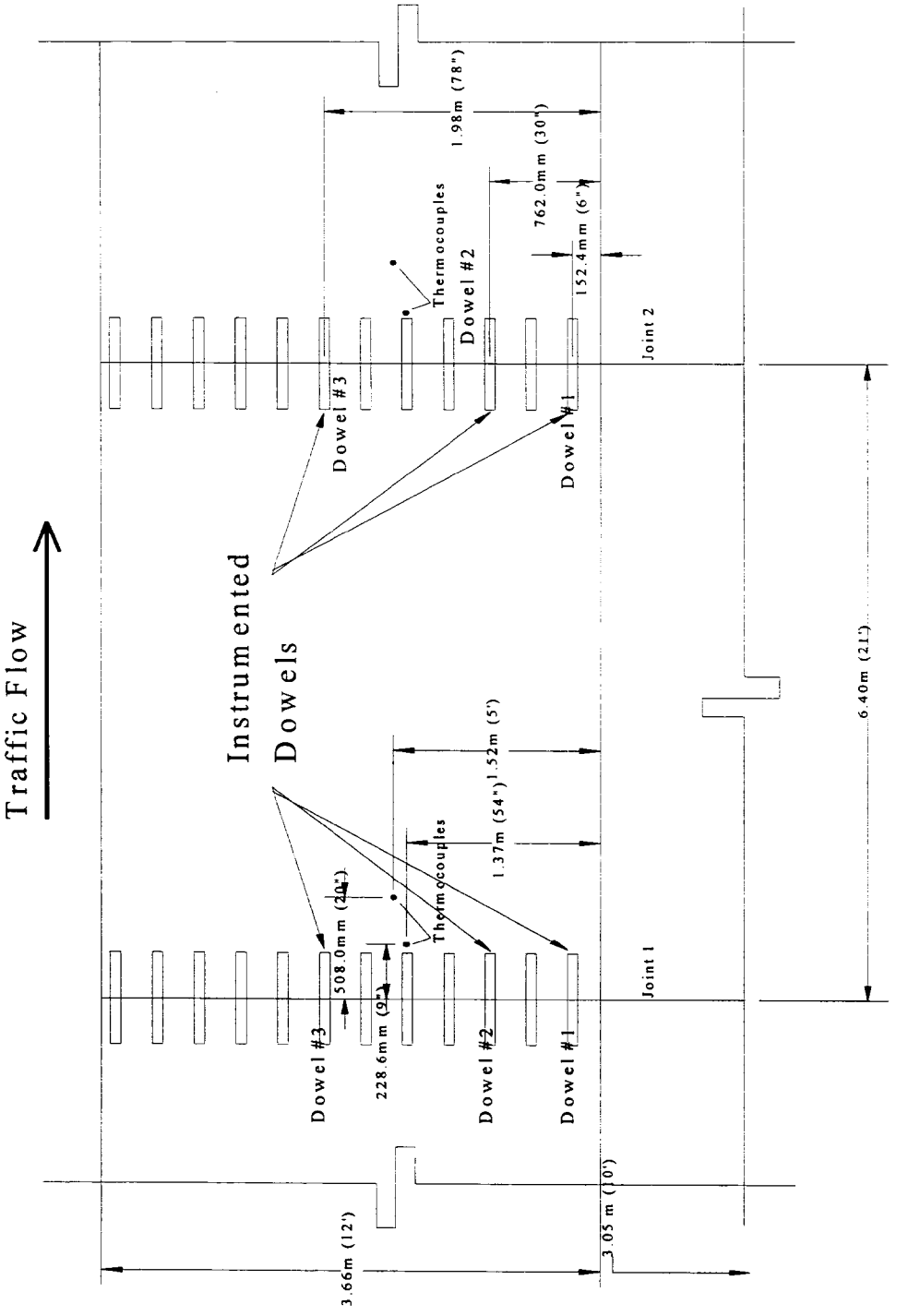

Figure 3.3 – Typical Section Instrumentation Plan

3.2 Slab Temperature

Two thermocouple units were installed to measure temperature in the concrete slab near each instrumented joint. One unit housed three sensors that measured temperature at 0 mm, 76 mm (3 in), and 152 mm (6 in) from the bottom of the concrete slab. The second unit consisted of a single sensor located 229 mm (9 in) from the bottom of the concrete slab. The three-sensor thermocouple units were attached to the dowel basket, 1.37 m (54 in) from the outside pavement edge and 229 mm (9 in) east of the joint, whereas the single sensor was placed 25 mm (1 in) deep in the green concrete, 1.52 m (5 ft.) from the outside pavement edge and 508 mm (20 in) east of the joint. The lead wire was laid in a groove and covered with concrete to protect it. Figure 3.3 shows the location of the thermocouples, and Figures 3.4 and 3.5 are photographs of the steel and fiberglass dowel baskets prior to placement of the concrete.

Figure 3.4 – Typical Steel Dowel Section

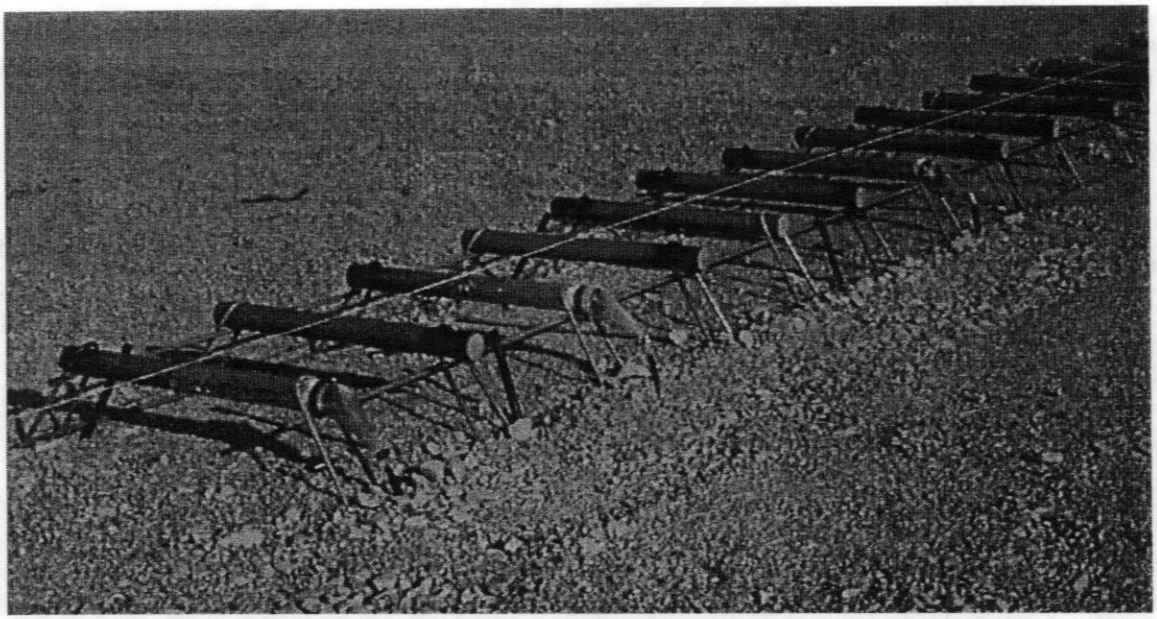

Figure 3.5 – Typical Fiberglass Dowel Section

3.3 Environmental Data Collection

The system used to automatically collect temperature and environmentally induced strain in the dowel bars at specified intervals of time consisted of a multiplexer, a CR7 measurement and control system manufactured by Campbell Scientific, Inc., and a laptop computer for downloading data and uploading programs. The function of the multiplexer was to increase the number of sensors that the CR7 datalogger could scan. It was positioned between the sensors and the datalogger, and mechanical relays were installed to switch the desired signals through the system.

The system collected data every 30 minutes for 37 days starting 1 hour before placement of the concrete so the full effect of curing could be recorded. Each data point collected was the average of five readings taken at 60 second intervals.

3.4 FWD Data Collection

The Ohio Department of Transportation provided a Dynatest Falling Weight Deflectometer (FWD) to apply dynamic loads at selected locations in the vicinity of the instrumented dowel bars as the sensor output was recorded. The recording system used to obtain dynamic strain gage output from the dowel bars read multiple channels and collected data at a rate of 400-500 samples/second/sensor during FWD loading. It consisted of a computer, a MEGADAC data acquisition system manufactured by Optim, and a MEGADAC expansion chassis. The system was activated as the FWD load was about to drop and turned off after impact. Three to four resonant FWD load pulses were typically recorded for each test.

FWD tests were performed in December 1997 when the pavement was new, and again in November 1999 after two years of service. The results of these tests are discussed in a later section.

3.5 Digital Filtering of Dynamic Data

It was not necessary to convert dynamic data obtained with the MEGADAC into strain values since the system collected, processed, and recorded the data in this form. However, the data still had to be filtered to remove "noise" caused by various forms of electrical interference. The filter was designed by the Kasier Window Method and was applied by fast convolution. It eliminated any noise not in the 45 to 55 Hz transition band without damaging the integrity of the collected data. Ohio University computer engineers wrote the filtering program specifically for strain data collected with the MEGADAC data acquisition system during FWD loading.

CHAPTER 4

DATA ANALYSIS

4.1 Introduction

The U.S. 50 high performance concrete pavement was monitored continuously to evaluate the curling and warping of PCC slabs caused by curing, and changes in environmental temperature and moisture. During pavement curing, temperature and moisture gradients resulting from the hydration process induced some initial permanent upward curvature of the slab ends. As seasonal and daily climatic cycles of temperature and moisture were superimposed on the pavement, slabs were exposed to subsequent curling and warping from differential expansion/contraction throughout their depth. Curling can be described as slab bending induced by temperature differences between the top and bottom fibers of the slab. In the same way, warping can be described as slab bending induced by moisture differentials in the slab. When temperature or moisture at the top of the slab is higher or lower than temperature or moisture at the bottom of the slab, it assumes the shape of a "frown" or "smile," respectively, in the longitudinal direction. This action of the slab causes dowels connecting the slabs to bend positively (in a "smile") or negatively (in a "frown") in a shape opposite that of the warped shape of the slab as they resist slab deformation. Stiffer dowel bars provide more resistance to this deformation, thereby creating higher stresses in the bars and in the concrete bearing against them.

4.2 Voltage to Strain Reduction

The uniaxial strain gages were set up in a half-bridge configuration and data were saved directly as strain. The equation which governs the behavior of a Wheatstone Bridge circuit, under initial balance conditions, for strain measurements is:

$$\Delta E = (V_o - V_I) = V \frac{R_1 R_2}{(R_1 + R_2)^2} \left(\frac{\Delta R_1}{R_1} - \frac{\Delta R_2}{R_2} + \frac{\Delta R_3}{R_3} - \frac{\Delta R_4}{R_4} \right) \qquad \textbf{Equation 1}$$

Where: ΔE = Change of voltage

R_1 = Strain gage resistance

$R_2 = R_3 = R_4$ = Resistance in other three arms of bridge

ΔR_1 = Change in strain gage resistance

V_o = Output voltage

V_I = Initial voltage

V = Excitation voltage

Since only one arm of the strain gage was active, the other three non-active arms produced no change in resistance. Also, it was assumed that the initial voltage in the circuit was zero, thereby reducing the above equation to:

$$V_o = V \frac{R_1 R_2}{(R_1 + R_2)^2} \left(\frac{\Delta R_1}{R_1} \right) \qquad \textbf{Equation 2}$$

Using the following electrical-resistance strain gage relationship:

$$\frac{\Delta R}{R} = G_f \varepsilon \qquad \textbf{Equation 3}$$

Where: ΔR = Change in strain gage resistance

R = Strain gage resistance

G_f = Gage factor supplied by the manufacturer

ε = Strain (expressed in micro-strain)

Substituting Equation 3 into Equation 2 and using the fact that R_1 is equal to R_2 produces the equation:

$$V_o = V \frac{G_f \varepsilon}{4} \qquad \textbf{Equation 4}$$

After a rearrangement of the equation and the addition of a factor to correct voltage for nonlinearity, as shown in Measurements Group Tech Note 507, the equation becomes:

$$\frac{V_o}{V} = \frac{G_f \varepsilon \times 10^{-3}}{4} \left(\frac{2}{2 + G_f \varepsilon \times 10^{-6}} \right) \qquad \textbf{Equation 5}$$

Nonlinearity errors occurring in conventional strain gage bridge circuits are normally small enough to ignore when measuring modest magnitudes of strain on elastic materials. They are included here, however, to improve overall accuracy of the resultant data. The final form of the equation is:

$$\varepsilon = \frac{4\left(\frac{V_o}{V}\right)}{G_f \left(1 \times 10^{-3} - \left(\frac{V_o}{V}\right) 2 \times 10^{-6} \right)} \qquad \textbf{Equation 6}$$

4.3 Dowel Bar Bending Moment

Strain measured by uniaxial gages on the top and bottom of the dowel bars was entered into the following equation for dowel bar bending moment:

$$M_z = \frac{EI(\varepsilon_b - \varepsilon_t)}{2c} \qquad \textbf{Equation 7}$$

Where: M_z = Moment in the z-axis of dowel

E = Young's Modulus of dowel

I = Moment of inertia of dowel ($\pi d^4/64$)

ε_b = Strain on bottom of dowel

ε_t = Strain on top of dowel

c = Distance from neutral axis

For this half-bridge strain gage configuration, direct strain readings were substituted for $(\varepsilon_b - \varepsilon_t)/2$ in Equation 7.

4.4 Dowel Bar Bending Stress

Maximum tensile and compressive bending stress in round dowel bars was determined from horizontal bending moments with the following equation:

$$\sigma = \frac{M_z c}{I} \qquad \textbf{Equation 8}$$

Where: M_z = Bending moment

c = Dowel radius

I = Moment of inertia of dowel

σ = Stress at the top and bottom of the dowel bar

4.5 Dowel Bar Shear

Since the two dominant forces placed on dowels by dynamic loading are bending moment about the z-axis and vertical shear, these values were considered more significant than horizontal shear, torque, and bending moment about the x-axis. Moments for both steel and fiberglass dowels were determined from Equation 7.

Equation 9 was used to calculate vertical shear forces from strain measured by the rosette gages as FWD loads were applied at the pavement joints:

$$P = \frac{3}{4} GA(\varepsilon_{side1} - \varepsilon_{side3})$$

Equation 9

Where: P = Vertical shear force

G = Shear modulus of dowel material

A = Cross-sectional area of dowel

ε_{side1} = Strain in leg of rosette directed 45 ° upward

ε_{side3} = Strain in leg of rosette directed 45 ° downward

Since strain gages do not measure vertical shear directly, the use of the above equation was necessary to relate strain recorded with the rosette gages to shear.

Shear stress on the dowels is the shear force divided by the cross-sectional area of the bar, as follows:

$$\tau = \frac{3}{4} G(\varepsilon_{side1} - \varepsilon_{side3})$$

Equation 10

Where, τ = Vertical shear stress

4.6 Concrete Bearing Stress

The actual bearing stress on concrete surrounding the dowel bars resulting from bending moments and shear in the dowel bars was calculated using the equation:

$$\sigma_b = K\left[\frac{P-\beta M}{2\beta^2 EI}\right] \qquad \textbf{Equation 11}$$

Where: σ_b = Bearing stress on the concrete

K = Stiffness of dowel support (assumed to be 900,000 pci)

P = Shear force on one dowel

M = Bending moment on dowel

$$\beta = \sqrt[4]{\frac{Kd}{4EI}}$$

Where: d = dowel diameter

E = Young's Modulus of dowel

I = Moment of inertia of dowel

The allowable bearing stress of concrete at the dowel bar surface was determined using the empirical equation:

$$f_b = \left(\frac{4-d}{3}\right)f_c' \qquad \textbf{Equation 12}$$

Where: f_b = Allowable bearing stress of concrete

d = Dowel diameter

f_c' = Compressive strength of concrete

CHAPTER 5

DISCUSSION OF RESULTS

5.1 Environmental Monitoring

Since the bending moment in dowel bars is zero prior to the time concrete is placed around them, obtaining absolute values for changes in moment over time requires that data collection begin before placement of the concrete. Even then, it is still difficult to isolate the specific changes in moment attributable to a single parameter since so many parameters (temperature, moisture, etc.) vary independently over time.

In Figure 5.1, the progressively higher average negative bending moments observed in the dowel bars during the first few days after placement of the concrete indicated a permanent upward curvature developing at the slab ends. Daily environmental cycles caused the slabs to deform around that initial set. Within a few days after concrete placement, peak bending moments in the steel dowel bars approached –200 N-m (-148 ft-lb), as shown. These data were calculated from Equation 7 using measured strain on the top and bottom of the dowel bars.

The -200 N-m (-148 ft-lb) bending moment was recorded at a time when the temperature on the pavement surface was 3^0C (5^0F) cooler than the bottom of the pavement. This moment was three-four times larger than that measured on the fiberglass dowels at the same time and with a similar temperature gradient in the slab (Figure 5.2). The larger moments in the steel dowels were attributed to their higher stiffness, which resisted slab curling to a greater degree than the fiberglass bars.

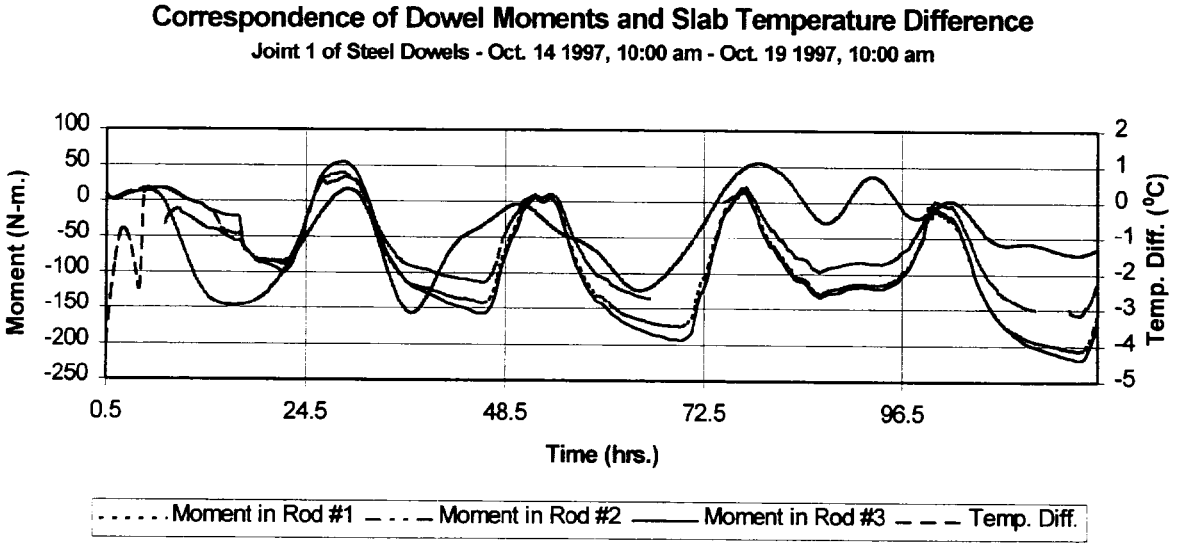

Figure 5.1 – Initial Steel Dowel Environmental Moment Data

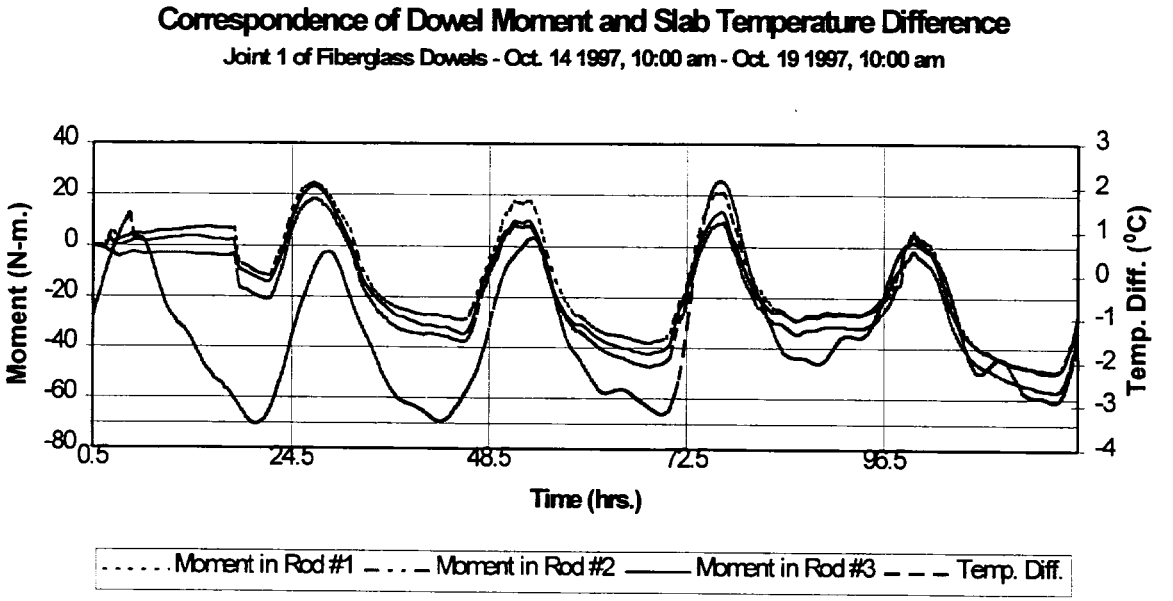

Figure 5.2– Initial Fiberglass Dowel Environmental Moment Data

From Equation 12, the allowable compressive bearing stress of the concrete was determined to be 17 MPa (2417 psi) after 7 days and 23 MPa (3333 psi) after 28 days. The concrete bearing stress calculated next to the steel dowel bars under an environmental bending moment of –200 N-m (-148 ft-lb) was 18 MPa (2600 psi) for the edge dowel, 16.5 MPa (2400 psi) for the wheelpath dowel, and 15.3 MPa (2225 psi) for the center dowel. The concrete bearing stress around the fiberglass dowel was much less at 3 MPa (450 psi) for the edge dowel, 4.5 MPa (650 psi) for the wheelpath dowel, and 4 MPa (560 psi) for the center dowel. These data suggest that high bearing stresses induced by steel dowel bars during the first few days after placement of the concrete may exceed the bearing capacity of the concrete at this early stage of hydration.

The maximum environmental concrete bearing stress of 32 MPa (4624 psi) calculated around steel bars in the wheelpath during these tests exceeded the allowable 28-day concrete bearing stress, but these levels were only observed at times when the temperature gradient changed 5^0C (9^0F) in 10 hours. This occurred about six times during the two-year test period and only in the edge and wheelpath dowels. The maximum bearing stress of 9 MPa (1280 psi) around fiberglass bars in the wheelpath was well under the allowable limit. Concrete bearing stresses induced by moving traffic loads add and subtract from these environmental stresses, depending upon the nature of the temperature gradient in the slab and the location of the wheel loads.

Using Equation 8, the bending stress in 1.5 inch diameter steel dowel bars under an environmental moment of –200 N-m (-148 ft-lb) was 36.9 MPa (5,280 psi). The corresponding stress in fiberglass bars under a moment of –45 N-m (-33 ft-lb) was 8.4 MPa (1,195 psi).

5.2 FWD Testing

5.2.1 Introduction

Falling Weight Deflectometer (FWD) testing serves many purposes, including:

1) Predicting long term pavement performance from measured deflections

2) Evaluating the efficiency of PCC joints in transferring dynamic load

3) Testing the operational status of dynamic sensors embedded in the pavement

4) Correlating dynamic deflections with sensor output

The FWD is one of the most widely used devices for non-destructive dynamic testing. Load pulses applied with the Dynatest FWD simulate the effect of a wheel load traveling at highway speed in both magnitude and duration. As an impulse load is applied via the 299.7 mm (11.8 in) diameter rubber plate, seven geophones mounted on the trailer record pavement surface deflection at various distances from the load plate. For these tests, the geophones were placed 0 mm, -304.8 mm (-12 in), 304.8 mm (12 in), 457.2 mm (18 in), 609.6 mm (24 in), 0.91 m (36 in), and 1.52 m (60 in) from the center of the plate. Surface deflections measured with these geophones are used to estimate the stiffness of individual pavement layers and the percent of load transfer across joints or cracks in rigid pavement.

Dynamic response of the dowel bars, vertical deflection of the slab ends, and load transfer across the joints were measured with the FWD load plate placed at the three locations shown in Figure 5.3. In the joint approach position, the joint was placed between the load plate and Sensor 3, and load transfer was calculated as (Df3/Df1) x 100 in percent. In the joint leave position, the joint was placed between the load plate and Sensor 2, and load transfer was calculated as (Df2/Df1) x 100, in percent. All deflections were normalized to a 1,000 lb. load for easier comparison of pavement responses, though this step was not necessary in the analysis of load transfer.

5.2.2 Dynamic Moment

An initial set of FWD measurements was obtained on December 3, 1997. During these measurements, several geophone readings were obviously in error. Those readings were removed and data appearing to be correct are shown in Appendix III. The FWD was upgraded in 1998 and a second set of readings was obtained on November 15, 1999. These data are also shown in Appendix III.

Loads were applied as the FWD load plate was placed near the joint on the approach side, as the FWD load plate was centered on the joint and as the FWD load plate was placed in the leave position just past the joint. The average magnitude of load used for analysis of the 1997 FWD tests was 57 kN (12,800 lbf) and the average slab temperature during testing was 2.8^{0}C (37^{0}F). Moments were calculated by inserting dynamic strain measured on the top and bottom of the dowel bars into Equation 7. Dynamic moments experienced by steel dowels in the wheelpath of Joint 1 were -16 N-m (-11.8 ft-lb) in the approach position, +46 N-m (+33.7 ft-lb) on the joint, and +42 N-m (+31.0 ft-lb) in the leave position. Moments measured in the approach, joint, and leave positions of Joint 1 in the section with fiberglass dowels were -29 N-m (-21.3 ft-lb), +3 N-m (+2.3 ft-lb), and +7 N-m (+5.2 ft-lb) respectively (see Figures 5.4 & 5.5 and Tables 5.1 & 5.2). The single highest moment was 69 N-m (51 ft-lb), which was on the departure side of a steel dowel joint.

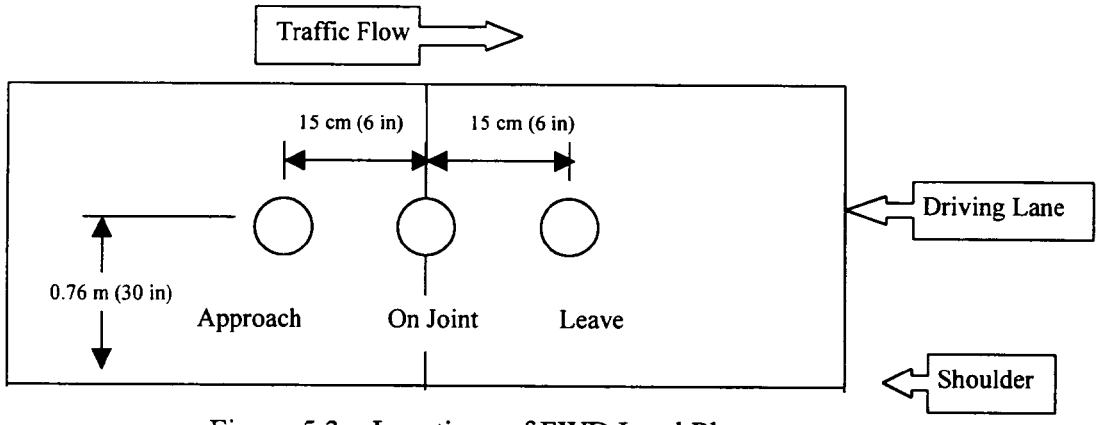

Figure 5.3 – Locations of FWD Load Plates

Unequal bending moments measured with the FWD on the approach and leave sides of the joints suggest that crack formation under the transfer saw kerfs was not perpendicular to the surface of the pavement. If a joint crack propagated vertically downward from the saw kerf, it would have gone through the center of the dowel bar at the gage, and moments measured on either side of a joint would be similar in sign and magnitude. Since data obtained at these locations showed dissimilar bending moments, it can be inferred that the cracks did not pass through the center of the dowel bars.

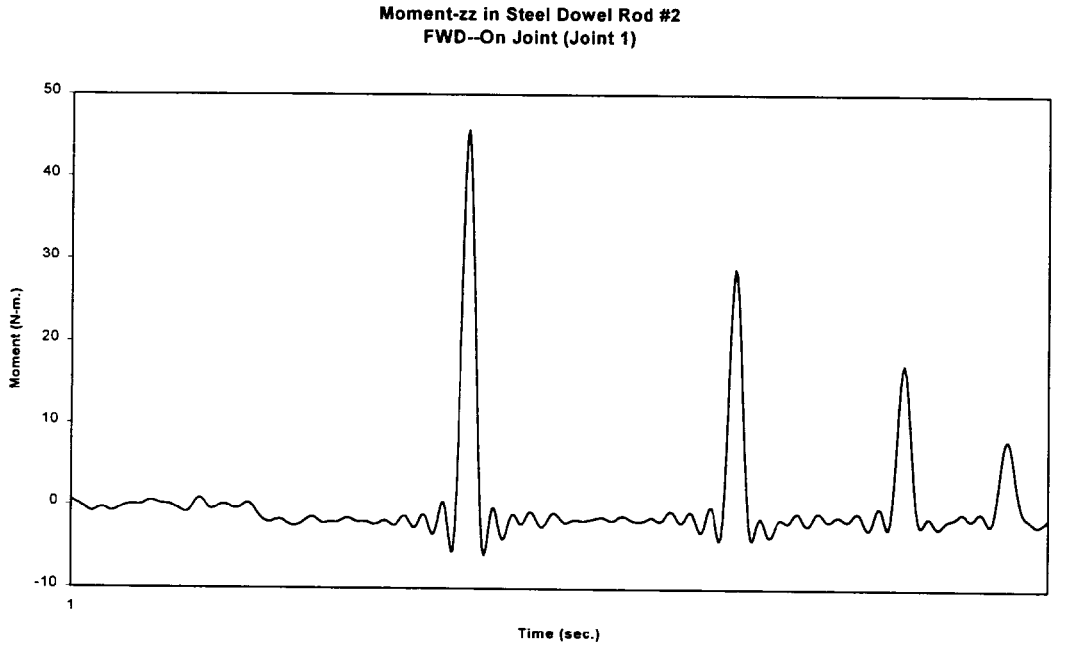

Figure 5.4 – Typical Steel Dowel FWD Moment Data

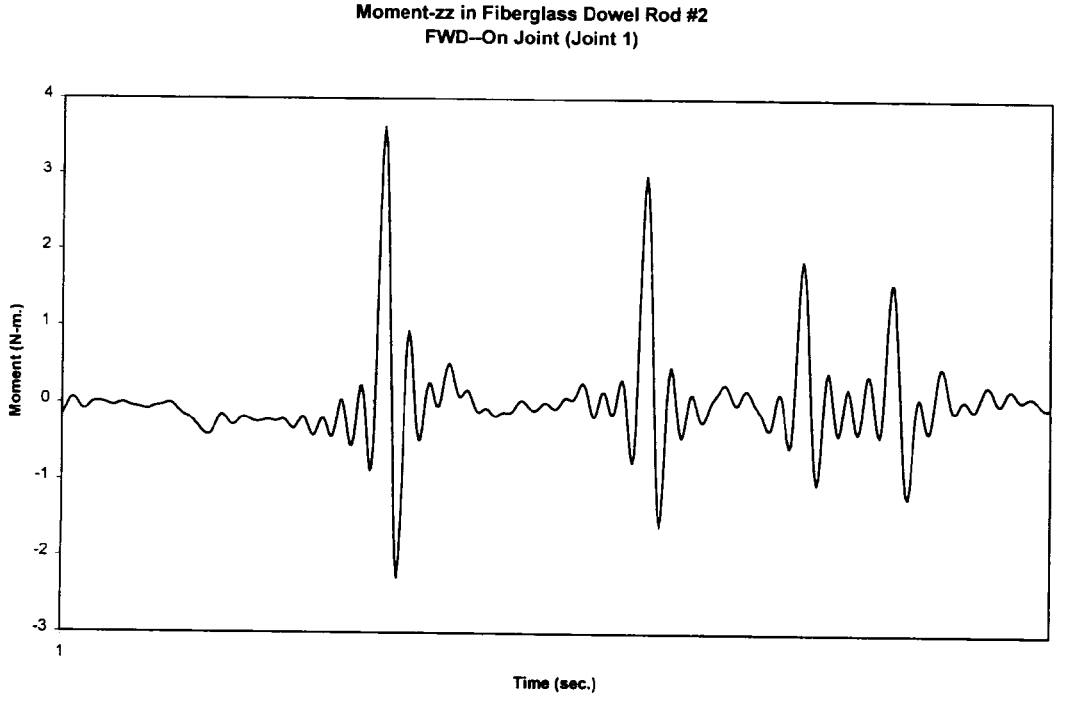

Figure 5.5 – Typical Fiberglass Dowel FWD Moment Data

Table 5.1 – Steel Dowel FWD Moment Results

Dowel Type: Steel @ 762 mm (30 in) Date: December 3, 1997 Average Slab Temp. 2.8° C (37° F) Joint 1				
Location of Drop	Force of Drop (kN)	Strain ($\mu\varepsilon$)	Moment (N-m)	Average Moment (N-m)
Approach	59.7	-15.17	-17.03	-15.62
Approach	58.8	-13.67	-15.35	
Approach	58.4	-12.88	-14.47	
On Joint	57.8	40.67	45.68	45.63
On Joint	57.1	40.70	45.71	
On Joint	56.9	40.50	45.49	
Leave	58.9	38.14	42.84	42.42
Leave	57.8	37.42	42.03	
Leave	57.1	37.73	42.38	

Table 5.2 – Fiberglass Dowel FWD Moment Results

Dowel Type: Fiberglass @ 762.0 mm (30 in) Date: December 3, 1997 Average Slab Temp. 2.8° C (37° F) Joint: 1				
Location of Drop	Force of Drop (kN)	Strain ($\mu\varepsilon$)	Moment (N-m)	Average Moment (N-m)
Approach	61.1	-97.75	-29.27	-28.83
Approach	61.1	-95.65	-28.65	
Approach	60.5	-95.39	-28.57	
On Joint	59.6	12.12	3.63	3.35
On Joint	59.8	12.62	3.78	
On Joint	60.2	8.86	2.65	
Leave	60.3	26.16	7.83	6.98
Leave	60.0	22.86	6.85	
Leave	59.3	20.90	6.26	

5.2.3 Dynamic Shear

As expected, vertical shear calculated in steel dowel bars with the FWD located at the on-joint position was much less than that at the approach and leave positions. The average magnitude of the steel dowel shear for all tests at the approach and leave positions was 2000 N (450 lbf), with a range of 1200 N (270 lbf) to 3500 N (787 lbf). Corresponding shear stresses for these magnitudes of total shear were 1754 KPa (254 psi), 1053 KPa (153 psi), and 3070 KPa (445 psi), respectively. On-joint shear was approximately 20% of these amounts. Data obtained during one set of FWD drops at one joint with steel dowels are shown in Figure 5.6 and Table 5.3.

Average shear in the fiberglass rods 152 mm (6 in) and 762 mm (30 in) from the pavement edge was 300 N (67 lbf) at the approach and departure locations, and 50 N (11 lbf) at the on-joint location, as shown in Table 5.4. Corresponding stresses for these shear forces were 262 KPa (38 psi) and 41 KPa (6 psi), respectively. Higher dowel moduli under dynamic load accounts for the larger shear stress measured in the steel dowel bars.

As in the case of bending moment, vertical shear should theoretically be the same at the approach and leave positions of the FWD. Shear data at these locations was also not equal which lends support to the earlier suggestion that the joint cracks did not propagate vertically downward through the center of the dowel bar.

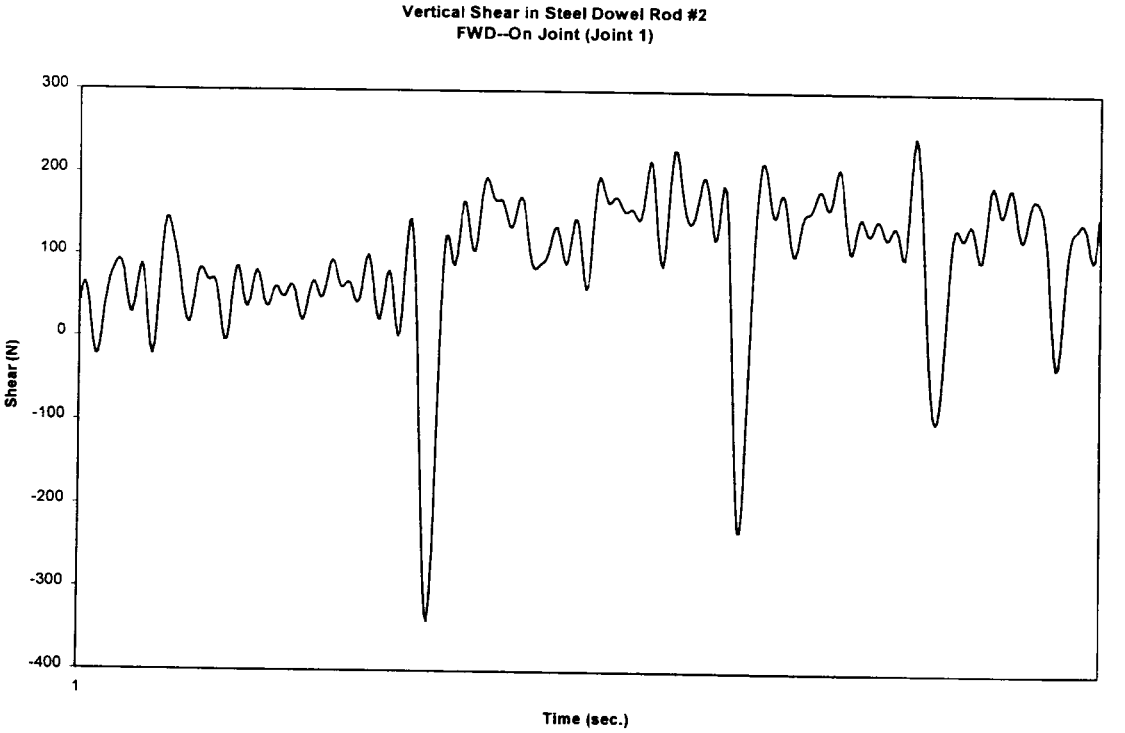

Figure 5.6 – Typical Steel Dowel FWD Shear Data

Table 5.3 – Steel Dowel FWD Shear Results

Dowel Type: Steel @ 762 mm (30 in) Date: December 3, 1997 Average Slab Temp. 2.8° C (37° F) Joint 1				
Location of Drop	Force of Drop (kN)	Strain ($\mu\varepsilon$)	Shear (N)	Average Shear (N)
Approach	59.7	-9.21	-1227	-1243
Approach	58.8	-9.48	-1244	
Approach	58.4	-9.43	-1257	
On Joint	57.8	-2.56	-341	-351
On Joint	57.1	-2.52	-336	
On Joint	56.9	-2.82	-376	
Leave	58.9	10.50	1399	1362
Leave	57.8	10.11	1347	
Leave	57.1	10.05	1339	

Table 5.4 –Fiberglass Dowel FWD Shear Results

Dowel Type: Fiberglass Date: December 3, 1997 Slab Temp. 2.8° C (37° F) Joint 1				
Location of Drop	Force of Drop (kN)	Shear in bar at 152 mm (6 in) from edge of pavement (N)	Shear in bar at 762 mm (30 in) from edge of pavement (N)	Shear in bar at 1.98 m (78 in) from edge of pavement (N)
Approach	61.1	-200	-300	-130
On Joint	59.8	-80	-20	-50
Leave	60.3	400	300	175

CHAPTER 6

CONCLUSIONS AND RECOMMENDATIONS

6.1 Summary

Dowel bars placed in PCC pavements to transfer forces across transverse contraction joints are exposed to various environmental and dynamic forces. Shortly after the placement of concrete and the sawing of joints over dowel bars, temperature and moisture gradients in the pavement typically cause the slab ends to curl upward as the concrete cures. During this hardening process, some residual curvature is set in the slabs. The direction and magnitude of this curvature is dependent upon temperature and moisture conditions present during the cure period. Rigid dowel bars at the joints resist this deformation through negative bending moments induced at the slab ends. The magnitude of these bending moments is dependent upon the stiffness of the dowel bars. Hveem (8) reported deformations of 0.25 inches in 20 foot slabs where dowel bars were bent and ruptured by fatigue. Therefore, dowel bars should be stiff enough to resist permanent deformation while yielding sufficiently to maintain acceptable levels of stress in the concrete. Environmental cycles cause continuous changes in slab curvature and dowel bar moments throughout the life of the pavement. Traffic loads add and subtract short-term dynamic stress to the total environmental stress.

Strain measurements in this study indicated that maximum bending moments of –100 Nm (-74 ft-lb), -150 Nm (-111 ft-lb), and –200 Nm (-148 ft-lb) were induced in the steel dowel bars one, two, and three days, respectively, after placement of the concrete. At three days, there was a permanent negative moment of about –100 to –150 Nm (-74 to –111 ft-lb) accumulated during curing, with a daily cycle of about $\pm$ 75 Nm (56 ft-lb) being superimposed as temperature fluctuated in the slab. Bending stresses in the steel bars corresponding to these maximum bending moments were 18.5 MPa (2,640 psi), 27.8 MPa (3,960 psi), and 36.9 MPa (5,280 psi), which are not excessive; and bearing stresses in the concrete surrounding the dowel bars were 9.0 MPa (1,300 psi), 13.5 MPa (1,950 psi), and 18.0 MPa (2,600 psi), respectively.

While 3 day compressive strengths were not available for the concrete, the allowable bearing stress at this time certainly would be less than the 17 MPa (2,417 psi) limit calculated from the 7 day compressive strength. A maximum environmental bearing stress of 32 MPa (4,641 psi) detected later in the tests also exceeded the allowable limit of 23 MPa (3,333 psi) calculated for concrete after 28 days. Considering the high concrete bearing stresses generated early by environmental factors alone and later by the combination of environmental factors and dynamic traffic loading, it would not be unreasonable to expect some progressive concrete deterioration at the dowel interface over time. This could result in looseness around the dowel bars and reduced efficiency in transferring forces across transverse joints.

For fiberglass bars, the maximum bending moments induced by initial slab curvature were –15 Nm (-11 ft-lb), -35 Nm (-26 ft-lb), and –45 Nm (-33 ft-lb) during the same three days after placement of the concrete. After three days, the permanent moment

was about –20 Nm (-15 ft-lb) with a daily cycle of ± 20 Nm (-15 ft-lb). These reduced moments were the result of lower dowel bar stiffness, which provided less resistance to slab curling. At a moment of – 45 Nm (-33 ft-lb), bending stress in the fiberglass dowel bars was 8.4 MPa (1,195 psi) and bearing stress in the concrete was 4.5 MPa (650 psi). A maximum bending moment of -84 Nm (-62 ft-lb) was observed in the fiberglass bars during these tests, resulting in a bending stress of 15.5 MPa (2,245 psi) in the bars and a bearing stress of 9 MPa (1,280 psi) in the concrete. The maximum allowable tensile and compressive bending stresses for these fiberglass bars are not known, but are assumed to be more than the measured stresses. For fiberglass dowels, bending stress in the bars appears to be a more important design consideration than bearing stress in the concrete.

As traffic loads pass over the pavement, dowel bars experience dynamic bending stresses that add to and subtract from the environmental stresses, depending upon the position of the vehicles. Using an FWD load of 57 kN (12,800 ft-lb), maximum dynamic bending moments varied from –16 Nm (-11.8 ft-lb) to + 46 Nm (+33.7 ft-lb) on the steel dowel bars and from –29 Nm (-21.3 ft-lb) to + 7 Nm (+5.2 ft-lb) on the fiberglass dowel bars. Again, these differences are caused by the differences in dowel bar stiffness. Non-uniformity of readings on both sides of the joints suggested that: 1) the saw joint did not crack vertically downward to the bottom of the pavement, and 2) slight variations in the location of the crack at the dowel bar and in the position of the dynamic load have significant impacts on bending moments in the dowel bars. Negative dynamic bending moments increase stresses in the dowel bars and surrounding concrete, while positive bending moments reduce these stresses. In either case, the dynamic bending stresses observed in these tests were minor when compared to the environmental bending stresses. When added together, however, the total bending stresses and the unknown impact forces caused by heavy traffic loads can result in significant bearing stresses on concrete surrounding dowel bars in PCC pavement.

Vertical shear in the steel dowel bars was calculated to be eight-nine times larger than vertical shear in the fiberglass dowel bars. The maximum shear measured on the steel bars was 3,500 N (787 lbf), which corresponded to a shear stress of 3,070 KPa (445 psi).

The U.S. 50 test pavement was placed in mid-October and the dynamic tests were conducted in December of that year, and November two years later. During these late fall and early winter months in Ohio, temperature gradients in rigid pavement slabs are generally quite modest, and yet, some high stresses were detected from slab curvature. It is possible that even higher stresses would be noted in the summer when more severe temperature and moisture gradients might exist during the early stages of concrete curing. It is also possible that there are particular conditions under which concrete placement should be avoided such as hot, sunny days with low humidity. Obviously, the economic and contractual pressures to complete projects on schedule currently have a higher priority than working around the weather to construct a better pavement, but there may be options available to mitigate some potentially serious problems once the mechanisms and interactions involving PCC design parameters, curing, and environmental conditions are more clearly understood.

6.2 Conclusions

Based upon data obtained from the instrumented dowel bars on U.S. 50 during environmental cycling in the field, the following conclusions can be made for steel and fiberglass dowel bars:

1. Steel dowel bars induced higher environmental bending moments across transverse PCC joints than fiberglass dowel bars.

2. Both types of dowels induced a permanent bending moment in PCC pavement slabs during curing. The magnitude of this moment appears to be a function of bar stiffness.

3. Curling and warping during the first few days after concrete placement can result in high bearing stresses being applied to concrete around the dowel bars. This stress may possibly exceed the allowable bearing stress of the concrete at that early age and result in some permanent loss of contact around the bars.

4. Data shown herein were obtained in the late fall and early winter months. High mid-summer temperature gradients in the pavement may result in even larger stresses being induced in the dowel bars and in the surrounding concrete, though concrete strength would also rise more rapidly during that time of the year.

Though no direct data were collected here on the permanent deformation of fiberglass dowels, there will likely be some creep over time.

Initial FWD testing took place on December 3, 1997, soon after construction was completed and when the weather was cold and wet. A second set of measurements was obtained on November 15, 1999. Based on the results of these tests, the following conclusions can be made regarding the dynamic response of steel and fiberglass dowel bars:

1. On this project, the magnitude of bending moments and vertical shear forces transferred by steel dowels across transverse PCC joints was much higher than for fiberglass bars of the same size.

2. The dynamic bending stresses induced in steel and fiberglass dowel bars by a 12,800 lbf FWD load were considerably less than environmental bending stresses induced by a 3 °C (5.4 °F) temperature gradient in these PCC slabs.

Based upon the combined results of dynamic and environmental testing, the following conclusions can be made:

1. During these tests, steel and fiberglass dowels both experienced higher moments from environmental factors than from dynamic loading.

2. The effects of environmental cycling and dynamic loading both must be included in the design and evaluation of PCC pavement joints.

3. In addition to transferring dynamic loads across PCC pavement joints, dowel bars serve as a mechanism to reduce the curling and warping of slabs due to curing, and temperature and moisture gradients in the slabs.

4. Because of the high bearing stresses that can be generated in concrete surrounding dowel bars, this parameter should be considered in dowel bar design, especially during the first few days after placement of the concrete.

6.3 Recommendations

Based upon the results obtained on U.S. 50, dowel bars in PCC pavement are subjected to large bending moments as the PCC slabs curl and warp during hydration and environmental cycling. These moments can translate into rather high bending stresses in the dowel bars, high bearing stresses in the concrete surrounding the dowel bars and significant bending stresses being introduced at the ends of the concrete slabs as curvature is resisted by the dowel bars. Moving traffic increases and decreases these stresses in complex cycles for short periods of time as vehicles traverse the slabs. These effects are not entirely accounted for in current rigid pavement design procedures. It must be remembered, however, that the data presented herein represents measurements from one dowel bar installation on one pavement with a single joint spacing and a nonstandard concrete mix. Dowel bars in other pavements may generate higher or lower internal stresses depending upon the various parameters involved.

The following three categories of recommendations are presented for consideration in improving the design of dowel bars in PCC pavement. First, is the need to instrument dowel bars in other PCC pavements to verify the U.S. 50 observations and to measure the effect of other design parameters on dowel bar performance. Second, is the need to model these field observations mathematically and to use this model for the optimization of dowel bar diameter, dowel bar spacing, joint spacing, etc. over a range of pavement thicknesses, material properties, and environmental conditions. Third, is the need to continue the search for alternative methods for reducing the internal stresses generated in PCC slabs.

Field Testing

- Instrument dowel bars in other PCC pavements to measure critical stresses generated during initial hydration, environmental cycling, and dynamic loading. Ideally, a number of sections could be included in one or two projects where the effect of other external variables would be uniform and monitoring would be more efficient. Specific variables of interest would include: pavement thickness, joint spacing, dowel bar diameter and spacing, and climatic conditions at the time of concrete placement.

Mathematical Modeling

- Review current procedures, including finite element techniques, for designing dowel bars in rigid pavement and assess their ability to predict critical stresses in the pavement structure during initial concrete hydration, environmental cycling and dynamic loading.

- Select the best technique available or develop a new technique that accurately models concrete and dowel bar stresses in rigid pavement structures over a range of design parameters and environmental conditions. Using this model, develop a procedure for designing dowel bars which considers, but is not necessarily limited to, bending stress in the dowel bars, bearing stress in the concrete surrounding the dowel bars, and bending stress induced in the concrete slab as it curls and warps during initial hydration and environmental cycling.

Minimization of Internal Stresses

- Explore innovative methods for reinforcing and curing PCC pavement slabs that reduce curling and warping during initial hydration and environmental cycling.

- Explore other dowel shapes, sizes, materials and spacing for the development of a more effective system to transfer load across PCC pavement joints.

APPENDIX I

REFERENCES

1. Ozbeki, M.A., Kilarski, W.P., and Anderson, D.A., "Evaluation Methodology for Jointed Concrete Pavements," *Transportation Research Record 1043*, TRB, National Research Council, Washington, D.C., 1985. pp. 1 – 8.
2. Colley, B.E., Tayabji, S.D., "Improved Rigid Pavement Joints," *Transportation Research Record 930*, TRB, National Research Council, Washington, D.C., 1983.
3. Timoshenko, S. and Ledels, J.M., "Applied Elasticity," Westinghouse Technical Night School Press, Pittsburgh, PA, 1925.
4. Friberg, B.F., "Design of Dowels in Transverse Joints of Concrete Pavement," *Journal of Transportation Engineering*, ASCE, Volume 105, 1979.
5. Tabatabaie-Raissi, A.M., "Structural Analysis of Concrete Pavement Joints," Ph. D. Dissertation, University of Illinois at Urbana-Champaign, 1978.
6. Vyce, J.M., "Performance of Load-Transfer Devices," Research Report 140, Engineering Research and Development Bureau, New York State Department of Transportation, July 1987.
7. Marcus, H., "Load Carrying Capacity of Dowels at Transverse Pavement Joints." *American Concrete Institute Journal*, ACI, Volume 48, 1952.
8. Hveem, F.N., "A Report on an Investigation to Determine Causes for Displacement and Faulting at the Joints in Portland Cement Concrete on California Highways," Materials and Research Department, State of California Division of Highways, May 17, 1949.

APPENDIX II

NOTATION

ΔE = Change of voltage

R_1 = Strain gage resistance

$R_2 = R_3 = R_4$ = Resistance in other three arms of bridge

ΔR_1 = Change in strain gage resistance

V_o = Output voltage

V_I = Initial voltage

V = Excitation voltage

ΔR = Change in resistance

R = Strain gage resistance

G_f = Gage factor supplied by the manufacturer

ε = Strain (expressed in micro-strain)

M_z = Moment in the z-axis of dowel

E = Young's Modulus

I = Moment of inertia

ε_b = Strain on bottom of dowel

ε_t = Strain on top of dowel

c = Distance from neutral axis (radius of dowel)

$V_y = P$ = Vertical shear force

Γ = Vertical shear stress

G = Shear modulus

A = Cross-sectional area of dowel

ε_{side1} = Strain in leg of rosette close to top

ε_{side3} = Strain in leg of rosette close to bottom

APPENDIX III

FWD LOAD TRANSFER MEASUREMENTS ON US 50

December 3, 1997

Load ~ 13,000 lbs.

Joint No.	Load Transfer (Df2/Df1) in %			Normalized Df1 in mils		
	Steel	Stainless	Fiberglass	Steel	Stainless	Fiberglass
1	83.4	80.4	78.0	0.43	0.45	0.52
2	53.3*	78.8	73.5	0.75*	0.45	0.57
3	81.1	84.8	61.7	0.47	0.40	0.51
4	80.1	79.1	84.5	0.38	0.40	0.34
5	79.6	77.0	78.9	0.44	0.46	0.40
6	86.0	80.3	68.0	0.37	0.40	0.37
Avg.	82.0	80.1	74.1	0.42	0.43	0.45

*Not included in the average. See Comment 4 below.

Notes:

1. In the FWD data header, the geophones were specified as being at 0, 12, 12, 18, 24, 36, and 60 inches. Because two geophones cannot be located at the same position, it was assumed that the second geophone was 12 inches behind the load plate or –12 inches.

2. These FWD data consisted of three drops at approximately 13,000 lbs. Load transfer and deflection normalized to 1,000 lbs. were calculated from the third drop unless the accuracy of these data was in doubt. When this accuracy was questionable, another drop was selected.

3. Some of the deflection data collected on December 3, 1997, appears to be incorrect. These errors fall into one of three general categories: a) Sensors Df2-Df7 being unreasonably high and somewhat random for a given drop, b) Sensor Df3 (and perhaps others) being too high or too low for all three drops at a given location, and c) one sensor being obviously incorrect for a given drop.

4. Only general observations should be made from the December 3, 1997 FWD data. Many readings were clearly incorrect and other errors not so obvious probably remain hidden in the data. Patterns observed in the data suggest that the problems were likely caused by a malfunction in the FWD. Data for Joint 2 in the section

with steel dowel bars were highly suspicious, and not included in the calculation of average load transfer or normalized deflection because Df1 was unreasonably high compared to the rest of the sensors at this location and the other Df1 readings in the three sections.

5. Based upon the averages calculated for load transfer and normalized deflection, and the uncertainties regarding the data, no significant differences can be identified between the three sections of pavement with different types of dowel bars.

November 15, 1999

Load ~ 10,000 lbs.

Joint No.	Load Transfer (Df2/Df1) in %			Normalized Df1 in mils		
	Steel	Stainless	Fiberglass	Steel	Stainless	Fiberglass
1	78.0	75.5	76.2	1.50	1.72	2.06
2	76.9	79.3	77.2	1.97	1.87	1.48
3	76.6	77.2	77.3	1.69	1.85	1.47
4	77.3	76.0	72.4	1.80	1.52	1.77
5	71.4	79.1	74.5	1.06	1.56	1.50
6	71.3	--	76.7	1.30	--	1.90
Avg.	75.3	77.4	75.7	1.55	1.70	1.70

November 15, 1999

Load ~ 13,000 lbs.

Joint No.	Load Transfer (Df2/Df1) in %			Normalized Df1 in mils		
	Steel	Stainless	Fiberglass	Steel	Stainless	Fiberglass
1	76.4	80.1	75.9	1.51	1.54	1.94
2	75.0	80.2	75.9	2.02	1.78	1.47
3	72.4	74.5	78.4	1.83	1.81	1.43
4	74.0	76.4	75.5	1.82	1.49	1.63
5	71.4	78.5	76.9	1.04	1.55	1.40
6	72.1	--	75.8	1.28	--	1.88
Avg.	73.6	77.9	76.4	1.58	1.63	1.63

Notes:

1. The 1999 data were collected with three drops, one drop each at approximately 10,000, 13,000, and 17,000 lbs. Data in the tables above are for the first two drops.

2. Average load transfer was essentially the same for all three types of dowel bars after two years of service.

3. Average normalized deflection under the load plate was somewhat lower for the steel dowel bars, but considering the variation existing within each set of joints

and the limited number of joints in each section, this difference is probably not significant.

4. Although four times higher in 1999, deflection under the load plate remained about the same for the three types of dowel bars. The change in deflection between 1997 and 1999 was probably caused by different temperature and/or moisture gradients within the PCC slabs, thereby resulting in distinctly different environmental slab curvatures at the time of the two FWD measurements.

Project: Performance of Dowel Bars and Rigid Pavement

A) Report Title: "Performance of Dowel Bars and Rigid Pavement"

Executive Summary

On U.S. 50, five-miles east of the City of Athens, the response of fiberglass, epoxy coated steel, and grout-filled stainless steel dowel bars were evaluated and compared under a variety of loading and environmental conditions. A few fiberglass and standard steel bars were instrumented to measure strain during curing, environmental cycling, and Falling Weight Deflectometer (FWD) loading.

Dowel bars were instrumented and installed at the time of construction of a Portland cement concrete (PCC) pavement containing 25% ground granulated blast furnace slag (GGBFS). Strain measurements were recorded for the dowel bars periodically over time to determine the forces induced during curing and during changes in environmental conditions, as well as dynamic loads applied with the FWD. Based upon data obtained from the instrumented dowel bars during environmental cycling in the field, steel dowel bars experienced higher bending moments across transverse PCC joints than fiberglass dowel bars. Both types of dowels experienced a permanent bending moment in the PCC pavement slabs during curing. The magnitude of this moment appears to be a function of bar stiffness. Curling and warping during the first few days after concrete placement can result in high bearing stresses being applied to the concrete around the dowel bars. This stress may possibly exceed the allowable bearing stress of the concrete at that early age and result in some permanent loss of contact around the bars.

Based on the results of the FWD tests, the magnitude of bending moments and vertical shear forces transferred by steel dowels across transverse PCC joints were much higher than for fiberglass bars of the same size. Overall, both steel and fiberglass dowels experienced higher moments from environmental factors than from dynamic loading.